to the precise ratio of CD_3OD to $CDCl_3$.) 9.16 (d, 1 H, J = 5.5), 8.68 (d, 1 H, J = 5.5), 8.66 (dd, 1 H, J_1 = 8.2, J_2 = 1.0 Hz), 8.31 (dd, 1 H, J_1 = 7.0, J_2 = 1.0 Hz), 7.97 (dt, 1 H, app $J_1 = J_2$ = 7.0, J_3 = 1.0 Hz), 7.88 (dt, 1 H, app $J_1 = J_2$ = 7.0 Hz, J_3 = 1.0 Hz), 6.92 (s, 1 H), 6.33 (dq, 1 H, J_1 = 7.0 Hz, $J_2 = J_3 = J_4$ = 1.4 Hz), 3.78 (t, 2 H, J = 6.7 Hz), 3.35 (t, 2 H, J = 6.7 Hz), 1.75 (t, 3 H, J = 1.2 Hz), 1.69 (dd, 1 H, J_1 = 7.0, J_2 = 1.0 Hz); ^{13}C NMR (2:1 $CD_3OD/CDCl_3$) 183.4, 170.5, 152.7, 149.9, 149.1, 146.0, 145.0, 127.2, 131.9, 131.5, 131.4, 131.1, 130.8, 129.7, 122.8, 121.4, 119.7, 117.7, 39.2, 30.8, 13.2, 11.6; IR (KBr) 3467, 3060, 2931, 1654, 1612, 1588, 1540, 1465, 1384, 1185, 862, 774; MS 359 (M^+ + 2), 357 (M^+), 272, 260, 247 (100), 218; HRMS expected 357.1477, obsd 357.1482.

Acknowledgment. The Robert A. Welch Foundation, the National Science Foundation, and the donors of the Petroleum Research Fund, administered by the American Chemical Society, provided financial support for these studies.

Registry No. 1, 113321-71-4; **2**, 113351-75-0; **3**, 113351-76-1; **9**, 128350-18-5; **10**, 42052-61-9; **11**, 135761-73-8; **12**, 135761-74-9; **13**, 135761-75-0; **14**, 4746-97-8; **15**, 51656-91-8; **16**, 62141-26-8; **17**, 135761-76-1; **18**, 32863-01-7; **19**, 128350-17-4; **20** (isomer 1), 135761-77-2; **20** (isomer 2), 135761-78-3; **21**, 135761-79-4; **22**, 135761-80-7; **29**, 135761-81-8; **30**, 128367-85-1; **31**, 128367-82-8; **32**, 128350-23-2; **33**, 128350-24-3; **34**, 128350-26-5; **35**, 128350-25-4; **36**, 135761-82-9; **37**, 128350-22-1; **38**, 135761-83-0; **44**, 135761-84-1; **45**, 135761-85-2; **46**, 135761-86-3; **47**, 135761-87-4; **48**, 135761-88-5; **49**, 135761-89-6; **50**, 135761-90-9; **51**, 135761-91-0; **52**, 135761-92-1; PhCHO, 100-52-7; CH_2=CHOEt, 109-92-2; o-$N_3C_6H_4CHO$, 16714-25-3; cyclohexanone, 108-94-1.

Diastereoselective Synthesis of Phycocyanobilin–Cysteine Adducts

John E. Bishop, Jon O. Nagy, John F. O'Connell, and Henry Rapoport*

Contribution from the Department of Chemistry, University of California, Berkeley, California 94720. *Received March 26, 1991*

Abstract: Methodology is presented for the synthesis of two diastereomers of a cysteine-linked phycocyanobilin derivative. The crucial reaction is a diastereoselective 1,6-Michael addition of cysteine methyl ester to an appropriate dihydropyrromethenone educt. The diastereomers so generated were then elaborated to two phycocyanobilin trimethyl esters. Definitive assignments of relative stereochemistry, double bond geometry, and solution conformation are accomplished by application of ROESY NMR experiments, while absolute stereochemical assignments are based on degradation to compounds of known chirality.

Introduction

Plant bile pigments, due to their extremely important photosynthetic and regulatory functions in numerous species, have been of considerable interest for well over 100 years. Such attention may also be, in part, a result of the pigments' brilliant and intense colors. The blue protein C-phycocyanin (C-PC), an antenna pigment isolated from the blue-green alga *Synechococcus* sp. 6301, was found to contain three distinct tetrapyrrole-based chromophores that are attached by thioether linkages to the protein, with a total molecular weight of approximately 36 700 Da.[1] Figure 1 depicts the structure that has been determined for the three identical phycocyanobilin (PCB) groups. NMR data from smaller peptide fragments determined the site of protein attachment to be C-3',[2] and when combined with data from appropriate synthetic model compounds,[3] showed a *trans*-dihydro relative stereochemistry at C-2 and C-3. However, the remaining stereochemical features of the molecule, namely the absolute stereochemistry assignments at C-2, C-3, and C-3', as well as the exocyclic double-bond geometries, were undetermined by this methodology. A recent X-ray crystal structure study on C-PC derived from *Mastigocladus laminosus* at 2.1-Å resolution convincingly assigned the absolute stereochemistry as 2*R*,3*R*,3'*R* for two of the chromophores, designated α-1 and β-1 PCB. The remaining PCB unit, β-2, was likewise assigned as 2*R*,3*R*,3'*R*; however, assignment of the C-3' stereocenter appears to be less convincing.[4,5] The X-ray diffraction data also showed *Z* double-bond geometries and an anti/syn/anti conformational relationship for the single bonds separating the four rings.

Scheme I. Cleavage of Phycocyanobilin from Phycocyanin

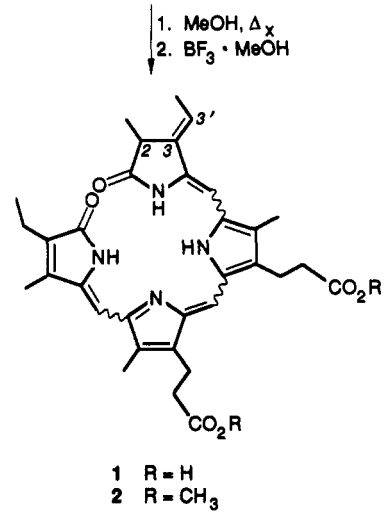

1 R = H
2 R = CH_3

Because of its chemical instability, as well as the presence of numerous stereochemical elements and complex functionalities, no total synthesis of a peptide-bound phycocyanobilin has been reported. Earlier studies concentrated primarily on the synthesis of natural product degradation products. Treatment with boiling methanol was found to cleave the tetrapyrrole–protein bond in an apparent elimination reaction, producing diacid **1** (Scheme I).[5-7]

(1) Glazer, A. N.; Fang, S. *J. Biol. Chem.* **1973**, *248*, 659.
(2) Lagarias, J. C.; Klotz, A. V.; Dallas, J. L.; Glazer, A. N.; Bishop, J. E.; O'Connell, J. F.; Rapoport, H. *J. Biol. Chem.* **1988**, *263*, 12977 and references cited therein.
(3) Schoenleber, R. W.; Kim, Y.; Rapoport, H. *J. Am. Chem. Soc.* **1984**, *106*, 2645.
(4) Shirmer, T.; Bode, W.; Huber, R. *J. Mol. Biol.* **1987**, *196*, 677.
(5) C-PC consists of two peptide chains, α and β. The use of α-1, β-1, and β-2 PCB refers to the three sites of chromophore attachment. In *Synechococcus* sp. 6301 C-PC, these designations correspond to the α chain's cysteine-84 residue and the β chain's cysteine-82 and cysteine-155 residues, respectively. See: Glazer, A. N. *Biochim. Biophys. Acta* **1984**, *768*, 29.
(6) Crespi, H. L.; Boucher, L. J.; Norman, G. D.; Katz, J. J.; Dougherty, R. C. *J. Am. Chem. Soc.* **1967**, *89*, 3642.
(7) Cole, W. J.; Chapman, D. J.; Siegelman, H. W. *J. Am. Chem. Soc.* **1967**, *89*, 3643.

0002-7863/91/1513-8024$02.50/0

Scheme II. Proposed Synthesis of Phycocyanobilin–Cysteine Adduct

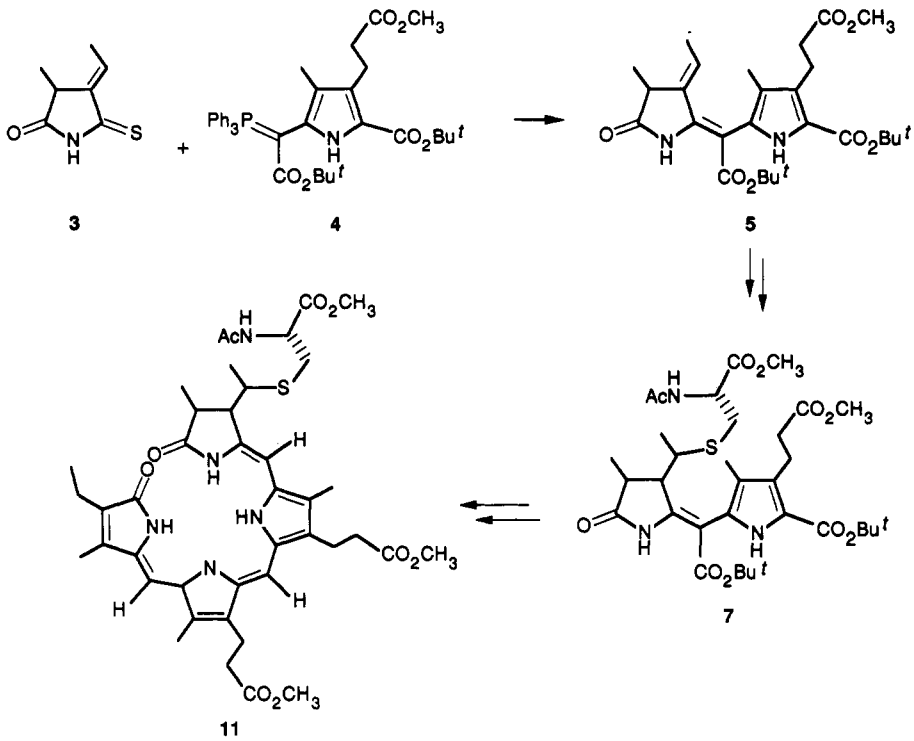

Subsequent esterification generated dimethyl ester **2**.[7] While the stereochemistry at C-2 and the double bonds remained undefined, the structure of **2** was confirmed by a racemic total synthesis.[8] Another study examined the synthesis of racemic *cis*- and *trans*-dihydro **2**, with saturation at C-3/C-3′.[3] The synthesis described now relies on suitably adapting these existing methodologies to the introduction of a cysteine substituent at C-3′.

Results and Discussion

Our projected synthesis for target molecule **11** is presented in Scheme II. The coupling of monothiosuccinimide **3**[9] and ylide **4** was recently described in an experimental and theoretical model study on the thio-Wittig reaction.[10] The presence of an ester group at the meso C-5 position of dihydropyrromethenone **5** was advantageous for several reasons. First, it was needed in order to construct a stabilized pyrrole ylide. More importantly, however, an electron-withdrawing group in this position would activate the ethylidene group and allow conjugate addition of a thiolate nucleophile (**5** → **7**) under mild conditions in a 1,6-Michael addition reaction. Finally, it was necessary for the group to be removable at a later stage in the synthesis, preferably under acidic conditions; alternate basic, reductive, and thermal conditions would not be compatible with the types of functionalities present. A *tert*-butyl ester best fit these criteria.

There is precedence for the conjugate addition of thiols in bile pigment chemistry. It has been hypothesized that PCB **1** biosynthetically adds to the cysteine residues of an apoprotein. This was recently mimicked in vitro, although the biosynthetic consequences of this study were not definitive.[11,12] Earlier, it was found that thiolate nucleophiles react with the ethylidene groups of 2-ethylidene-3-methylsuccinimide[13] and phycocyanobilin dimethyl ester **2**,[14] although the latter adduct was not structurally characterized. Addition to the former compound was reported to give exclusively trans stereochemistry for the ring substituent. This was also supported by the report that addition of methanol to PCB dimethyl ester **2** gave exclusively the trans ring substituent stereochemistry.[15]

Our initial synthetic probes involved the addition of L-cysteine methyl ester to a racemic mixture of pyrromethenone **5** (Scheme III) in the presence of a catalytic amount of 1,8-diazabicyclo-[5.4.0]undec-7-ene (DBU). At 0 °C in acetonitrile, the reaction was complete within 30 min. A total of four diastereomers was produced in a ratio of 21/5/1/14 and were labeled **6A**, **6B**, **6C**, and **6D**, respectively. The addition reaction produced two product-containing bands by TLC. The higher R_f band contained **6A** and **6B**, while the low R_f band contained **6C** and **6D**. These sets of diastereomers were separated by chromatography and then treated with acetic anhydride. Purification of the resulting product mixtures by chromatography allowed isolation of the four diastereomerically pure, spectroscopically distinct *N*-acetyl derivatives **7A**, **7B**, **7C**, and **7D**.

Diastereoselectivity in the addition reaction appears to be governed by the chirality at C-2.[16] Addition at C-3′ takes place

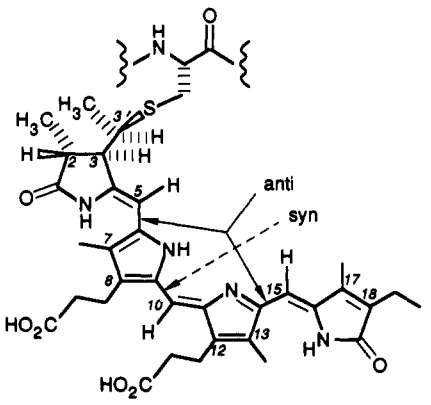

Figure 1. Structure of the PCB chromophore in C-Phycocyanin as determined by X-ray crystallography.[4]

(8) Gossauer, A.; Hinze, R.-P. *J. Org. Chem.* **1978**, *43*, 283.
(9) Bishop, J. E.; Dagam, S. A.; Rapoport, H. *J. Org. Chem.* **1989**, *54*, 1876.
(10) Bishop, J. E.; O'Connell, J. F.; Rapoport, H. *J. Org. Chem.* **1991**, *56*, 5079.
(11) Arciero, D. M.; Bryant, D. A.; Glazer, A. N. *J. Biol. Chem.* **1988**, *263*, 18343.
(12) Arciero, D. M.; Dallas, J. L.; Glazer, A. N. *J. Biol. Chem.* **1988**, *263*, 18350.
(13) Klein, G.; Rüdiger, W. *Liebigs Ann. Chem.* **1978**, 267.
(14) (a) Klein, G.; Rüdiger, W. *Z. Naturforsch.* **1990**, *45C*, 1099. (b) Lüönd, E. B.; Köst, H.-P.; Rüdiger, W. *Z. Naturforsch.* **1990**, *45c*, 1099.
(15) Gossauer, A.; Hinze, R.-P.; Kutschan, R. *Chem. Ber.* **1981**, *114*, 132.

Scheme III. Conversion of Pyrromethenone **5** to Bilin–Cysteine Adduct

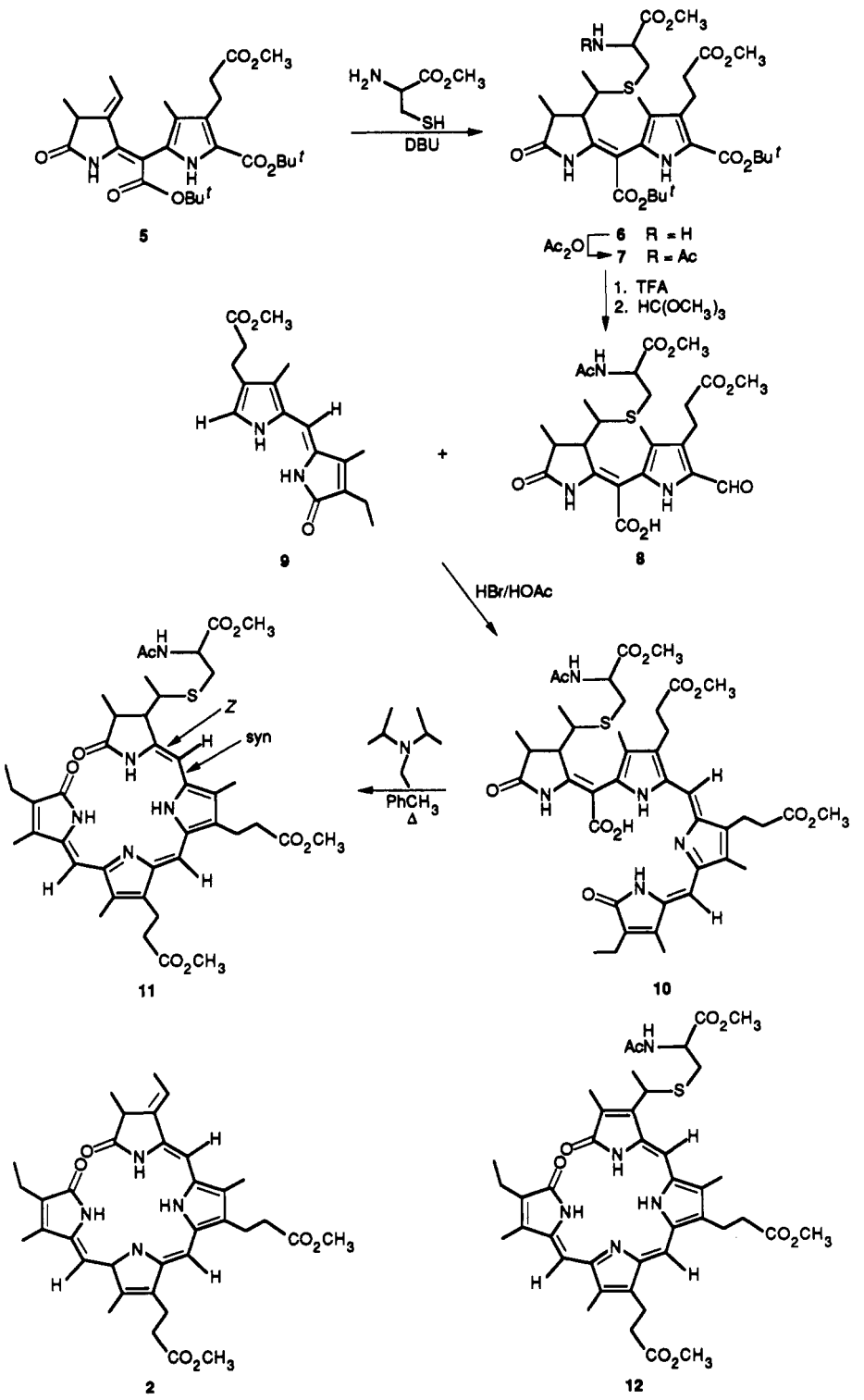

on the side of the double bond opposite the adjacent C-2 methyl group. Scheme IV depicts the addition of cysteine to the 2*R* enantiomer of **5**. Attack would occur on the β face of the double bond, producing a 3′*R* configuration. Reprotonation then favors a trans relationship of substituents at C-2 and C-3, producing a 2*R*,3*R*,3′*R* arrangement. Because racemic **5** was used, the 2*S* enantiomer of **5** was also present, producing a 2*S*,3*S*,3′*S* configuration. Appendage of chiral cysteine made these two adducts separable as the two major diastereomers **7A** and **7D**. Data supporting these stereochemical assignments were accumulated after elaboration to the tetrapyrroles and are presented later in this discussion.

The nature of the two minor diastereomers was not as readily interpretable. Since partial racemization of cysteine could lead to the formation of undesirable stereoisomers, a series of control experiments was conducted in which L-cysteine methyl ester and (*S*)-ethyl-L-cysteine methyl ester[17] were treated with DBU at 0 °C and at 24 °C. The recovered amino esters were analyzed for

(16) Adherence to pyrromethenone nomenclature is not observed. For clarity, we have used a numbering scheme analogous to that of the subsequent tetrapyrrole. IUPAC convention is followed for designation of relative stereochemistry: *Pure Appl. Chem.* **1976**, *45*, 13. Phycocyanobilin contains a 3,3′-unsaturation and refers to the pigment released from the native phycocyanin as shown in Scheme I.

(17) Zahn, H.; Traumann, K. *Liebigs Ann. Chem.* **1953**, *581*, 168.

Scheme IV. Stereochemical Path of Cysteine Addition to Pyrromethenone **5**

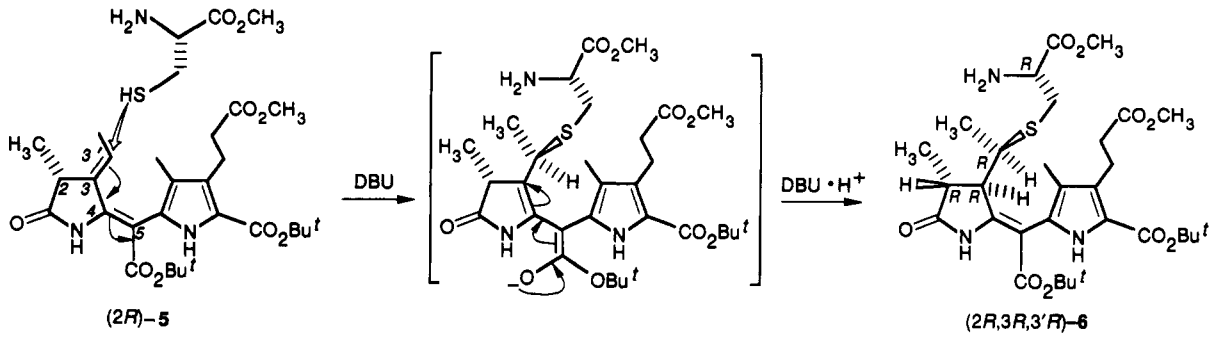

optical purity by coupling to both L- and DL-*N*-(phenylsulfonyl)proline acid chloride[18] followed by HPLC separation of the diastereomers. Complete retention of optical activity was demonstrated for the two amino esters at both temperatures.

Another hypothesis for the presence of two minor isomers centers around the possibility of incomplete stereocontrol in the conjugate addition reaction. This could arise from three conceivable causes. The first possibility, initially considered the most likely, involved nucleophilic attack on the disfavored face of the double bond at C-3′, resulting in diastereomers 2*R*,3*R*,3′*S* and 2*S*,3*S*,3′*R*. These assignments, however, were not consistent with further chemical and spectroscopic observations. A second possibility was that the minor diastereomers resulted from partial meso C-4/C-5 double bond isomerization from the *Z* to the *E* configuration.[19] Rotation of the lower order C-4/C-5 bond of the conjugate addition intermediate (see Scheme IV) could occur before reprotonation takes place, resulting in double bond isomerization. Thirdly, two minor diastereomers could also arise if reprotonation afforded products with a cis relative stereochemistry at C-2 and C-3. Because of severely overlapping ^{1}H NMR resonances, it proved impossible to verify the exclusive obtention of trans C-2/C-3 relative stereochemistry for all four diastereomers at the dihydropyrromethenone stage. However, NMR data from the subsequent tetrapyrroles clearly showed a trans substituent pattern.

These hypotheses also had to account for one important observation: diastereomers **7B** and **7D** provided spectroscopically indistinguishable tetrapyrroles. This would necessitate that a configurationally labile element of stereochemistry equilibrates minor diastereomer B to major diastereomer D, or vice versa, under the subsequent reaction conditions. Two potentially labile elements of stereochemistry are the meso double bond and the C-3 center. After later removal of the *meso-tert*-butyl ester, complete isomerization of the double bond was observed. It is possible, for example, that **7D** had a stereochemistry of 2*S*,3*S*,3′*S*-4*Z* and **7B** had a stereochemistry of 2*S*,3*S*,3′*S*-4*E*, and that after removal of the *meso-tert*-butyl ester, thermodynamic equilibration of the double bond produced identical diastereomers. However, this was considered highly unlikely. The starting material **5** was previously shown to have a complete preference for the C-4/C-5 *Z* configuration under these reaction conditions. Photoisomerization of the C-4/C-5 double bond to the *E* configuration followed by treatment with catalytic DBU or trifluoroacetic acid (TFA) at 0 °C resulted in rapid and complete isomerization back to the *Z* isomer.[10] This preference is believed to result from strong hydrogen bonding forces between pyrrolic NH's and the meso carboxyl group, which presumably exist in both the starting material and the Michael adducts. It was also observed that the *E* isomer of **5**, lacking internal hydrogen bonding, was more polar than the *Z* isomer and had a correspondingly lower R_f value by TLC. Since diastereomer B, before acetylation, had a significantly higher R_f value than diastereomer D, a double bond assignment of *E* for diastereomer B would be qualitatively inconsistent with these results. Despite repeated attempts, the presence of the bulky *meso-tert*-butyl ester group made it impossible to directly assign the double bond geometry of the cysteine adducts by NMR techniques.

The most likely explanation for these observations involves partial obtention of cis substituents at C-2 and C-3 upon reprotonation. The C-3 position is unquestionably the most configurationally labile stereocenter in the molecule. This was demonstrated by a vexing side reaction, β-elimination of the peptide from the pyrrole nucleus, which occurred at both the di- and tetrapyrrole stages under acidic or basic conditions. It is therefore quite conceivable that the major diastereomer **6D** had a 2*S*,3*S*,3′*S* configuration and that the minor diastereomer **6B** had a 2*S*,3*R*,3′*S* configuration. Subsequent elaboration to the tetrapyrrole could then equilibrate the stereochemistry of B to the more thermodynamically favored *trans*-dihydro stereochemistry of D. No unambiguous experiments, chemical or spectroscopic, could be devised to test this hypothesis, and unfortunately, minor diastereomer **6C**, while similarly expected to equilibrate to diastereomer **6A**, could not be obtained in enough quantity to generate a sample of tetrapyrrole product suitable for definitive spectroscopic studies. As a result of these findings, subsequent discussion and experimental details are confined to the two major diastereomers, **7A** and **7D**.

Given the high diastereoselectivity in the addition of cysteine to racemic **5**, complete diastereospecificity would be achieved if educt **5** could be synthesized in enantiomerically pure form. This would require obtaining optically active monothiosuccinimide **3** (Scheme II), which was accomplished by coupling racemic **3**[9] to L-*N*-(phenylsulfonyl)proline acid chloride,[18] giving a mixture of diastereomers that were readily separated by preparative HPLC and then hydrolyzed to optically active **3**. Unfortunately, the chiral center in monothiosuccinimide **3** proved to be extremely labile, and loss of optical integrity occurred rapidly upon storage. As expected, the subsequent thio-Wittig reaction gave material with essentially no optical activity.

For the purpose of producing alternate diastereomers of phycocyanobilin, an attempt was also made to isomerize the C-3/C-3′ ethylidene double bond of **5** from *E* to *Z*. Addition of cysteine would then presumably result in diastereomers epimeric at C-3′ (i.e., 2*R*,3*R*,3′*S* instead of 2*R*,3*R*,3′*R*). Since the *Z* isomer of monothiosuccinimide **3** is thermodynamically less stable and would readily isomerize to the *E* isomer,[8] we attempted to isomerize the ethylidene double bond of **5**. Irradiation of **5** isomerized the meso double bond, but exposure to catalytic DBU was found to rapidly regenerate the preferred *Z* isomer,[10] and addition of L-cysteine methyl ester to the isomerization product produced an identical diastereomer composition.

With the major diastereomers **7A** and **7D** in hand, the next step entailed *tert*-butyl ester cleavage, decarboxylation, and formylation, which was done by sequential treatment with TFA and trimethyl orthoformate, followed by an aqueous workup. Surprisingly, the meso carboxyl group, a vinylogous carbamic acid, did not de-

(18) Maurer, R. J.; Takahata, H.; Rapoport, H. *J. Am. Chem. Soc.* **1984**, *106*, 1095.

(19) Adherence to substituent priority rules is observed for *E*/*Z* double bond assignments. This is somewhat misleading in that a *Z* C-4/C-5 (meso) double bond in pyrromethenone **5** and a *Z* geometry for target molecule **11** (after the meso ester group is removed and decarboxylated) correspond to trans and cis double bond arrangements, respectively, relative to the position of ring nitrogen atoms around the double bond.

Scheme V. Synthesis of Pyrrolinone **16**

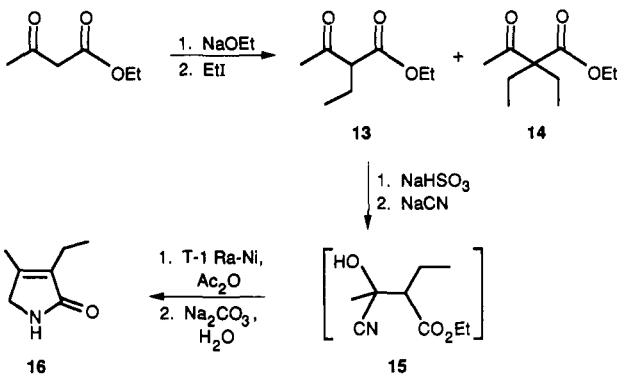

carboxylate. Under more forceful reaction conditions, decarboxylation could be accomplished, but this was always accompanied by β-elimination of the amino acid. ^{1}H NMR spectroscopic analysis of crude acid **8A** suggested that partial double bond isomerization had occurred; however, attempted purification under both normal- and reverse-phase conditions proved difficult and resulted in substantial losses of material. The crude acids were therefore used directly in the next reaction.

The synthesis of pyrromethenone **9**[3] and its precursors[3,10] has been previously discussed. However, in this present study several important modifications of these existing procedures, namely in the synthesis of the D-ring precursor, pyrrolinone **16**, were employed (Scheme V). The first reaction, alkylation of ethyl acetoacetate, has always been a problematic step, mainly due to purification difficulties in separating mono- and dialkylated products. While this separation can be tediously performed by spinning-band distillation, the resulting fraction of monoalkylated **13** always contained about 15–20% dialkylated material **14**. The reaction mixture was purified by chromatography much more efficiently, and on a 1-mol scale, 52% of **13** was isolated containing less than 2% of the dialkylated product. Cyanohydrin formation was accomplished by treatment of **13** with sodium bisulfite and sodium cyanide with methodology previously described,[20] and the crude material was used directly in the next reaction.

Reduction of the cyanohydrin nitrile functionality has, in our hands, been the most troublesome and scale-limiting step in the sequence, requiring Raney nickel (of unspecified grade) with high temperatures (>100 °C) and high pressures (>1500 psi). Initial attempts to effect this reduction with alternate catalysts under less vigorous conditions failed. We found that freshly generated T-1 Raney nickel[21] would indeed reduce cyanohydrin **15** at 50 psi and 33 °C in acetic anhydride. Critical to this procedure was that the crude cyanohydrin be pretreated with a batch of catalyst, which was removed by filtration. A fresh aliquot of catalyst was then added and hydrogenation proceeded smoothly. After the crude hydrogenation product was refluxed in water with Na_2CO_3, a variation of the final purification conditions afforded highly pure pyrrolinone **16** in a yield of 29% from **13**. This revised sequence is superior to that previously described in yield, ease of operation, and adaptibility to scaleup.

Information related to the double bond geometry of pyrromethenone **9**[3] was also obtained. This type of compound has frequently been written, for convenience, showing *E* geometry, because no direct proof of structure had been reported. A phase-sensitive NOESY[22] NMR experiment, however, clearly proved *Z*-syn geometry. Dipole–dipole exchange was observed between the two NH protons. Exchange between the meso proton and the pyrrolic methyl groups was also observed.

The acid-mediated coupling of diastereomeric formyl dihydropyrromethenones **8A** and **8D** to pyrromethenone **9** (Scheme III) produced diastereomeric tetrapyrrolecarboxylic acids **10A** and **10D**. Once again, chromatographic purification proved ineffective. Suitable purification, however, could be performed with a separatory funnel. It was observed that acid **8** could be extracted into an aqueous bicarbonate phase, while **10** remained in the organic phase. Use of a slight excess (110 mol %) of **8** forced the bimolecular coupling reaction to completion, and excess **8** was then washed away into the weakly alkaline aqueous phase. The ^{1}H NMR spectrum of acid **10A** isolated from this extraction procedure was quite clean, but an impurity, appearing to be approximately 10% of a diastereomer and perhaps the result of partial C-4/C-5 double bond isomerization, was carried into the final reaction. The UV–vis spectra of the purple-colored diastereomers **10** showed absorption maxima at 332 and 572 nm in methanol and 326 and 597 nm in 10 mM aqueous TFA. In natural product derived bilipeptides, the visible absorption maximum is at approximately 650 nm in acidic media.[11,23] This discrepancy must be the result of an electronically or conformationally induced effect of the C-5 carboxylate group.

The last step of the synthesis, decarboxylation at C-5, proved to be a most challenging reaction. In acidic media, the dominant reaction pathway was β-elimination followed by decarboxylation, affording released phycocyanobilin dimethyl ester **2**. In basic and neutral media, elimination and oxidation of the A ring to a less saturated pigment **12** were the predominant pathways. Finally, a procedure was adapted that had been successful for decarboxylation of a pyrrole derivative with a carboxylic acid in the β-position, also formally a vinylogous carbamic acid.[24] Heating a toluene solution of acid **10A** to 105 °C in the presence of triethylamine primarily produced side product **2**, but small quantities of target compound **11A** were detected. Use of a more sterically hindered base, diisopropylethylamine, almost completely suppressed the elimination side reaction, and **11A** was obtained as the major product. Purification of the decarboxylated tetrapyrroles was accomplished by silica gel chromatography. Removal of the high R_f elimination product **2**[8] was straightforward. Product **11** was not particularly stable on the chromatographic support, and the highest yields were obtained when a minimum quantity of silica gel was used with fast elution. Unfortunately, separating the somewhat variable quantities of the slightly higher R_f, blue-colored oxidation product **12** from purple-colored **11** sometimes required larger quantities of support and slower elution. Isolated yields of **11** ranged from a modest, but reproducible, 20–30% on small-scale reactions (<100 mg) to 70–90% with larger scale reactions when little of contaminant **12** was formed.

Numerous attempts were made to inhibit the oxidative side reaction. Adding antioxidants to the reaction mixture appeared to have no effect. The best results were obtained when the reaction was conducted under an atmosphere of argon. Although the desired material **11** could be purified to homogeneity by properly cutting chromatographic fractions, it proved impossible to amass large enough quantities of pure oxidation product **12** for complete spectroscopic characterization. A mixed fraction containing approximately a 1/1 mixture of **11A** and **12A** was therefore analyzed. In methanol, the oxidized material exhibited an absorption maximum around 650 nm, approximately 60 nm longer in wavelength than **11**. Analysis of the mixture by fast atom bombardment (FAB) mass spectrometry showed a protonated parent molecular ion peak at 790 Da, two mass units less than that observed for **11**. The ^{1}H NMR spectrum was complicated due to the presence of two compounds; however, it was clear that the added unsaturation was at C-2/C-3. An additional methyl singlet was observed in $CDCl_3$ at 1.93 ppm for the 2-CH_3, and the 3′-CH_3 resonance was at 1.64 ppm, shifted 0.23 ppm downfield from the corresponding resonance in the saturated derivative. Additionally, the structure assignment and spectroscopic data of **12A** were consistent with the recently described report of mesobiliverdin-type pigments.[11,12]

(20) Gossauer, A.; Weller, J.-P. *Chem. Ber.* **1978**, *111*, 486.
(21) Dominguez, X. A.; Lopez, I. C.; Franco, R. *J. Org. Chem.* **1961**, *26*, 1625.
(22) Bodenhausen, G.; Kogler, H.; Ernst, R. R. *J. Magn. Reson.* **1984**, *58*, 370.
(23) Bishop, J. E.; Lagarias, J. C.; Nagy, J. O.; Schoenleber, R. W.; Rapoport, H.; Klotz, A. V.; Glazer, A. N. *J. Biol. Chem.* **1986**, *261*, 6790.
(24) Carter, P.; Fitzjohn, S.; Halazy, S.; Magnus, P. *J. Am. Chem. Soc.* **1987**, *109*, 2711.

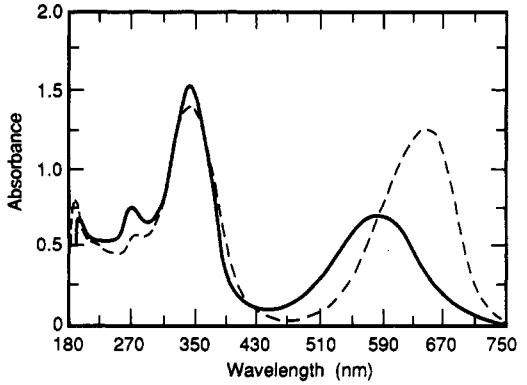

Figure 2. UV-vis spectra of **11A** in methanol (—) and in 10 mM aqueous TFA (---) at 23 °C.

Finally, attempts were made to hydrolyze the methyl ester groups of **11** in order to obtain materials more closely resembling the free acid natural product. Once again, removal of the esters was accompanied by elimination under forceful acidic conditions and oxidation under alkaline conditions. Since the products and intermediates appear to be quite stable in acidic media at moderate temperatures (<30 °C), the use of esters that are more acid-labile probably could avoid these problems.

Characterization of Synthetic Bilin–Cysteine Adducts via UV–Vis Spectroscopy. UV-vis spectra of diastereomer **11A** in methanol and 10 mM aqueous TFA are presented in Figure 2. Absorbance maxima and extinction coefficients for **11D** were identical. In methanol, the ratio of the near-UV peak at 345 nm to the visible maximum at 590 nm was 2.2/1. The previously reported model compound, with a hydrogen atom replacing cysteine at C-3′, had the visible absorbance maximum at 583 nm.[3] This 7-nm difference may result from a cysteine-induced conformational effect. With **11A** in 10 mM aqueous TFA, these maxima were observed at 347 and 647 nm, the visible peak being more intense and shifted 57 nm to the red of the peak observed in methanol. The ratio of near-UV to visible peaks was 1.1/1. These data are nearly identical with values observed for bilipeptides obtained from the tryptic digestion of C-phycocyanin, where, for example, absorbance maxima at 345 and 646 nm were reported for β-1 PCB in 10 mM aqueous TFA.[11] Differences have been observed between these tryptic bilipeptides and the native protein C-PC in terms of absorption and fluorescence emission spectra, and it has been speculated that these differences result from alternate conformations of the bilin groups.[11,25]

NMR Spectroscopy of Bilin–Cysteine Adducts. ^{1}H NMR spectra of **11A** and **11D** were recorded in both $CDCl_3$ and pyridine-d_5; the data are presented in Tables I and II. All assignments were verified by examining scalar couplings derived from phase-sensitive COSY experiments[22,26] (data not presented) and dipole–dipole interactions. Because previous NMR analyses of natural product derived bilipeptides were performed in pyridine-d_5,[2] the data in Table II were most relevant. Having relatively large amounts of synthetic material in hand resulted in spectra of high signal-to-noise ratios, and allowed resolution enhancement by use of a squared sine bell apodization. In this way, very precise assignments of all coupling constants could be made. Salient among these were the 3-H/5-H allylic coupling constants (1.2–1.5 Hz), the 2-H/3-H coupling constants (5.3 Hz) proving a *trans*-dihydro relative stereochemistry for both diastereomers,[3] and the 3-H/3′-H coupling constants (3.5–3.9 Hz). In $CDCl_3$, the latter value was 5.1 Hz for **11A** and 3.4 Hz for **11D**. These 3-H/3′-H coupling constants had never been determined for the natural products[2] and were of value, as will be described shortly, in assigning the conformation around the C-3/C-3′ bond and the relative stereochemistry at C-3′.

(25) Nesvadba, P.; Gossauer, A. *J. Am. Chem. Soc.* **1987**, *109*, 6545.
(26) Marion, D.; Wüthrich, K. *Biochem. Biophys. Res. Commun.* **1983**, *113*, 967.

Table I. ^{1}H NMR Spectral Assignments of **11A** and **11D** in $CDCl_3$

	11A		11D	
assignment	chem shift	mult	chem shift	mult
cys N-H	7.16	d, 7.4	7.04	d, 7.8
10-H	6.67	s	6.67	s
15-H	5.99	s	5.98	s
5-H	5.59	s	5.63	d, 1.4
cys α-H	4.74	dq, 7.0, 4.4	4.76	dq, 7.0, 4.9
OCH_3	3.74	s	3.68	s
OCH_3	3.68	s	3.66	s
OCH_3	3.67	s	3.61	s
3′-H	3.25	dq, 6.7, 5.1	3.32	dq, 7.0, 3.4
cys β-CH(1)	3.09	dd, 13.9, 4.2	3.10	dd, 13.3, 4.8
cys β-CH(2)	3.02	dd, 13.9, 6.7	3.03	dd, 13.1, 7.0
12-$CH_2CH_2CO_2CH_3$	2.94	t, 7.7	2.94	t, 7.6
8-$CH_2CH_2CO_2CH_3$	2.90	t, 7.7	2.90	t, 7.7
3-H	2.84	br t, 4.2	2.99	br t, 5.1
12-$CH_2CH_2CO_2CH_3$	2.55	t, 7.7	2.55	t, 7.5
8-$CH_2CH_2CO_2CH_2$	2.55	t, 7.7	2.54	t, 7.7
2-H	2.55[a]	*a*	2.64	dq, 7.4, 5.1
18-CH_2CH_3	2.29	q, 7.5	2.32	q, 7.4
17-CH_3	2.12	s	2.13	s
13-CH_3	2.11	s	2.11	s
7-CH_3	2.02	s	2.03	s
cys N-$COCH_3$	1.92	s	2.01	s
3′-CH_3	1.41	d, 6.9	1.39	d, 6.9
2-CH_3	1.21	d, 7.4	1.24	d, 7.3
18-CH_2CH_3	1.07	t, 7.5	1.10	t, 7.6

[a] Precise assignment was not possible because of overlapping resonances.

Table II. ^{1}H NMR Spectral Assignments of **11A** and **11D** in Pyridine-d_5

	11A		11D	
assignment	chem shift	mult	chem shift	mult
N-H	11.18	br s	9.85	br s
cys N-H	9.31	d, 7.8	9.37	d, 8.0
10-H	7.04	s	7.04	s
15-H	6.07	s	6.08	s
5-H	5.83	d, 1.5	5.87	d, 1.2
cys α-H	5.20	dq, 7.7, 5.7	5.25	dq, 7.8, 5.1
OCH_3	3.65	s	3.60	s
OCH_3	3.60	s	3.58	s
OCH_3	3.58	s	3.57	s
3′-H	3.60[b]	*b*	3.60[b]	*b*
cys β-CH(1)	3.34	dd, 13.6, 5.5	3.38	dd, 13.6, 5.2
cys β-CH(2)	3.25	dd, 13.6, 7.6	3.12	dd, 13.6, 8.2
3-H	3.16	ddd, 5.3, 3.9, 1.5	3.21	ddd, 5.3, 3.5, 1.6
12-$CH_2CH_2CO_2CH_3$	3.04	t, 7.3	3.05	t, 7.4
8-$CH_2CH_2CO_2CH_3$	2.95	t, 7.6	2.96	t, 7.5
2-H	2.80	dq, 7.7, 5.2	2.80	dq, 7.3, 5.3
12-$CH_2CH_2CO_2CH_3$	2.67	t, 7.7	2.68	t, 7.2
8-$CH_2CH_2CO_2CH_3$	2.64	t, 7.7	2.64	t, 7.5
18-CH_2CH_3	2.48	m	2.47	m
17-CH_3	(2.08)[c]	s	(2.10)[c]	s
13-CH_3	(2.07)[c]	s	(2.08)[c]	s
cys N-$COCH_3$	2.04	s	(2.07)[c]	s
7-CH_3	1.99	s	2.00	s
3′-CH_3	1.50	d, 6.9	1.49	d, 7.0
2-CH_3	1.41	d, 7.3	1.42	d, 7.4
18-CH_2CH_3	1.23	t, 7.5	1.23	t, 7.5

[a] Precise coupling constants were determined from a squared sine bell apodization. [b] Precise assignment was not possible because of overlapping resonances. [c] Resonances were too close in chemical shift to distinguish by 2-D methods.

With the exception of the three methyl ester singlets, subsequent dipole exchange experiments allowed the assignment of all resonances in $CDCl_3$. This included differentiation of the three pyrrole methyl singlets, 7-, 13-, and 17-CH_3's, as well as the 8- and 12-propionyl side chains.

Because of their increasingly recognized relationship to absorption and fluorescence characteristics, it was viewed as espe-

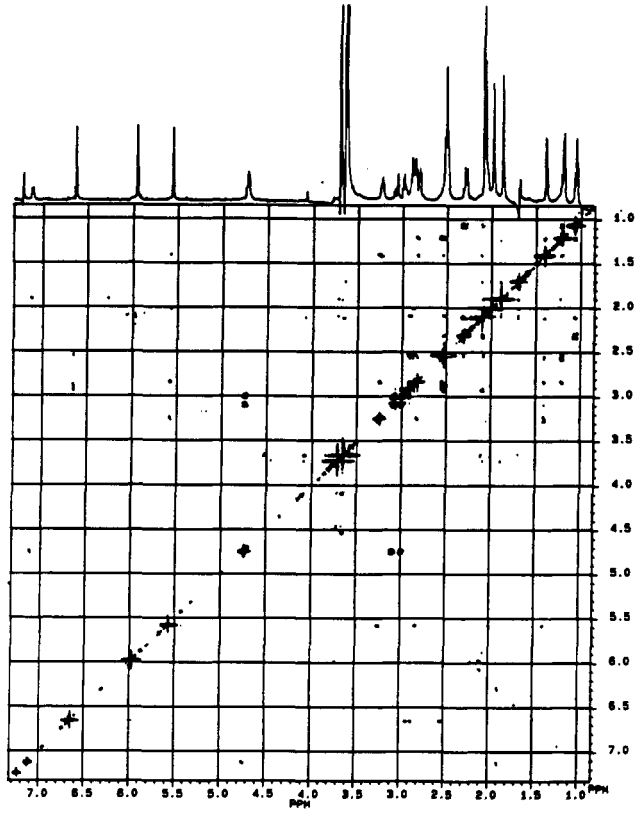

Figure 3. ROESY and 1-D ^{1}H NMR spectra (2K resolution) of **11A** in $CDCl_3$.

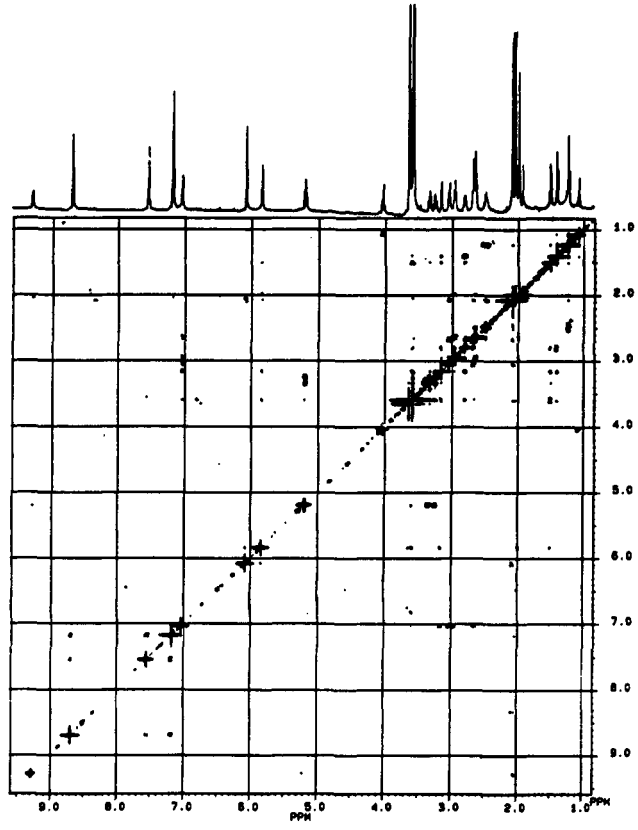

Figure 4. ROESY and 1-D ^{1}H NMR spectra (2K resolution) of **11A** in pyridine-d_5.

cially important that suitable methodology be implemented to delineate the synthetic compounds' configurational and conformational properties in solution. This type of information is commonly gained by examining through-space dipolar coupling between nuclei with NOESY NMR techniques. While we previously had used these experiments with natural product derived bilipeptides, information was confined to location of the peptide–bilin linkage.[2] In attempting to further exploit this methodology with the synthetic materials, no cross peaks could be observed from the phase-sensitive NOESY experiment. This was especially surprising because we were able to use a mixing time (250 ms) that had been optimized with the higher molecular weight natural products, and we had virtually unlimited quantities of material available: the sample concentrations of natural product derived bilipeptides were approximately 1 mM, while 60 mM solutions of the synthetic materials were used.

The reason for the lack of cross peaks was that molecules of this size (ca. 800–1000 Da) typically have correlation times, τ_c (time for 2π molecular rotation), such that at high magnetic field strength, τ_c equals the inverse Larmor frequency of the protons ($1/\omega_0$). In these cases, the laboratory frame or longitudinal cross relaxation rate is very small or zero. Thus, cross peak intensities in the NOESY spectra of these molecules are very small, making structural assignments difficult or impossible. In contrast, rotating frame or transverse cross relation rates are never zero and are monotomically increasing for increasing correlation time.[27] Thus, cross relaxation in the rotating frame does not have difficulties with some correlation time regions as does the laboratory frame of the NOESY experiment. The experiment that allows for mixing in the rotating frame is the rotating frame Overhauser Effect spectroscopy (ROESY) experiment, which uses a spin-lock field to allow for transverse relaxation.[28]

In order to make relative stereochemical assignments of the synthetic diastereomers, ROESY cross peak intensities were correlated to interatomic distances by developing a computer program that simulated NOESY/ROESY 2-D intensity maps as a function of field strength, correlation time, interatomic distances, laboratory or rotating frame relaxation, nuclei type, and mixing time for multiple spin systems.[29] The computational method was based on the solution to the relaxation master equation in matrix form.[27,30] Experimental τ_1 and τ_2 values were used to adjust the leakage rates to fit experimental data. Thus, for a given mixing time, a set of force field calculation derived interatomic distances were correlated to experimental NOESY/ROESY intensity data.

Accordingly, ROESY data from both diastereomers were acquired in $CDCl_3$ (Figure 3) and pyridine-d_5 (Figure 4). Table III lists observed dipole–dipole interactions. In general, pyridine-d_5 spectra exhibited longer range interactions than those acquired in $CDCl_3$. Data from **11D** were virtually identical with those obtained from **11A** and are therefore not illustrated. The discussion that follows represents an analysis of data derived from **11A** in pyridine-d_5. Explicit mention of **11D** in pyridine-d_5, **11A** in $CDCl_3$, or **11D** in $CDCl_3$ is made only when significant differences from **11A** in pyridine-d_5 were observed. Although symmetrized 2-D plots are illustrated, analysis and comparison of spectra were accomplished by careful examination of unsymmetrized 2-D and cross-sectional data. The results of these experiments, when compared to those from the unsuccessful NOESY experiment, were quite dramatic, as strong cross peaks were observed. Computer modeling allowed systematic analyses of the data and was advantageous in raising for consideration various combinations of configuration and conformation that otherwise may not have been apparent. The high sensitivity of the experiment allowed definitive assignments of relative stereochemistry, double bond geometry, and solution conformation.

Assignments of double bond geometry and conformation at the meso (C-5, C-10, and C-15) positions were made by examining

(27) Solomon, I. *Phys. Rev.* **1955**, *99*, 559.
(28) See: Kessler, H.; Bats, J. W.; Griesinger, C.; Koll, S.; Will, M.; Wagner, K. *J. Am. Chem. Soc.* **1988**, *110*, 1033.
(29) Macura, S.; Huang, Y.; Suter, D.; Ernst, R. R. *J. Magn. Reson.* **1981**, *43*, 259.
(30) (a) Jeener, J.; Meier, B. H.; Bachmann, P.; Ernst, R. R. *J. Chem. Phys.* **1979**, *71*, 4546. (b) Macura, S.; Ernst, R. R. *Mol. Phys.* **1980**, *41*, 95.

Table III. Dipole Exchange Cross Peaks Observed for **11A** in Pyridine-d_5 and $CDCl_3$

resonance	interacting resonances
cys N-H	cys α-CH, cys N-$COCH_3$
10-H	8- and 12-$CH_2CH_2CO_2CH_3$, 8- and/or 12-$CH_2CH_2CO_2CH_3$
15-H	17-CH_3, 13-CH_3
5-H	3′-H, 3-H, 7-CH_3, 3′-CH_3 (weak)
cys α-CH	cys N-H, cys β-CH(1), cys β-CH(2)
3′-H	5-H, cys β-CH(1),[a,b] cys β-CH(2),[a,b] 3-H,2-H (weak),[b] 3′-CH_3, 2-CH_3 (weak)
cys β-CH(1)	cys α-CH, cys β-CH(2), 3′-H,[a,b] 3-H,[a,b] 3′-CH_3 (weak)
cys β-CH(2)	cys α-CH, cys β-CH(1), 3′-H,[a,b] 3-H[a,b]
12-$CH_2CH_2CO_2CH_3$	10-H, 12-$CH_2CH_2CO_2CH_3$, 13-CH_3
8-$CH_2CH_2CO_2CH_3$	10-H, 8-$CH_2CH_2CO_2CH_3$, 7-CH_3
3-H	5-H, 3′-H, cys β-CH(1),[a,b] cys β-CH(2),[a,b] 2-H, 3′-CH_3, 2-CH_3
12-$CH_2CH_2CO_2CH_3$	10-H, 12-$CH_2CH_2CO_2CH_3$, 13-CH_3
8-$CH_2CH_2CO_2CH_3$	10-H, 8-$CH_2CH_2CO_2CH_3$, 7-CH_3
2-H	3′-H (weak),[b] 3-H, 3′-CH_3 (weak), 2-CH_3
18-CH_2CH_3	17-CH_3, 18-CH_2CH_3
17-CH_3	15-H, 18-CH_2CH_3, 18-CH_2CH_3[b]
13-CH_3	15-H, 12-$CH_2CH_2CO_2CH_3$, 12-$CH_2CH_2CO_2CH_3$
7-CH_3	5-H, 8-$CH_2CH_2CO_2CH_3$, 8-$CH_2CH_2CO_2CH_3$
cys N-$COCH_3$	cys N-H
3′-CH_3	5-H (weak), 3′-H, cys β-CH(1) (weak), 3-H, 2-H (weak), 2-CH_3[a]
2-CH_3	3′-H (weak),[b] 3-H, 2-H, 3′-CH_3[a]
18-CH_2CH_3	18-CH_2CH_3, 17-CH_3

[a] A cross peak was observed, but because the resonances were so close in chemical shift, it was impossible to distinguish T_1 noise from actual dipole–dipole exchange. [b] Not observed in $CDCl_3$ spectrum.

the interaction of the vinylic protons with surrounding groups. Cross peaks can be seen between 5-H and the 3′-H, 3-H, and 7-CH_3 resonances, mandating a *Z* geometry of the C-4/C-5 double bond and a syn conformation for the C-5/C-6 single bond. The 10-H resonance exchanges with both the 8- and 12-propionyl side chains, likewise indicating a *Z*-syn arrangement between the B and C rings. Because the 13-CH_3 and 17-CH_3 resonances of **11A** in pyridine-d_5 were too close in chemical shift to be differentiated at the 2-D spectral resolution (4.3 Hz/point), it could not be determined from these data if 15-H was interacting with both or just one of the pyrrole methyl singlets. The high intensity of the cross peak suggested both. However, in $CDCl_3$, the two singlets were far enough apart to observe the interaction of both with 15-H and allow a *Z*-syn assignment between the C and D rings.

Assignments of *trans*-dihydro (2*R**,3*R**)[16] relative stereochemistry at C-2 and C-3, made earlier for both diastereomers by examination of the coupling constants, were corroborated by the ROESY interactions. It should be noted that strong dipole–dipole exchange was observed between 2-H and 3-H. Because the two nuclei are well within the range of observable dipole exchange in both relative configurations, this does not necessarily lead to a cis assignment. Instead, more distance-sensitive interactions must be observed. The combination of a relatively strong 3′-H/2-H cross peak and a very weak 3′-H/2-CH_3 cross peak (unobservable for **11D**) confirmed the 2*R**,3*R** relative orientation for both diastereomers.

Attention was then focused on determining the relative stereochemistry between C-3 and C-3′. This task was much more difficult than determination of the C-2/C-3 relationship because one must consider variations of conformation as well as configuration. A thorough review of the data left no doubt that the C-3/C-3′ relative stereochemistry was 3*R**,3′*R** for both synthetic diastereomers. This assignment was based primarily on three sets of interactions: (1) The 5-H/3′-H cross peak was very intense and considerably stronger than 5-H/3′-CH_3, (2) the 2-H/3-H interaction was much stronger than 2-H/3′-H; and (3) the 3′-CH_3/3-H interaction was more intense than 3′-CH_3/2-H.

As an example of how calculated distance geometries were used in assigning the relative stereochemistry at C-3′, Figure 5 shows

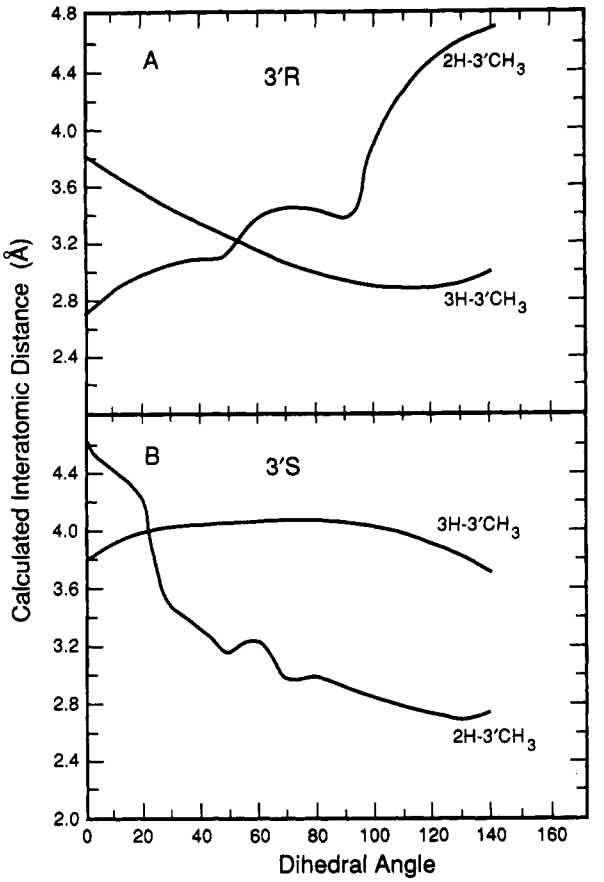

Figure 5. 2-H/3′-CH_3 and 3-H/3′-CH_3 interatomic distances as a function of dihedral angle (3′-H/C-3′/C-3/3-H) for (A) the *R* configuration at C-3′ and (B) the *S* configuration at C-3′.

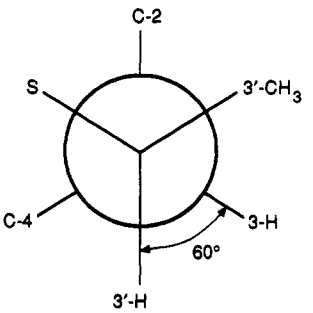

Figure 6. Newman projection of the C-3′/C-3 bond, shwoing a 3*R*,3′*R* configuration with a 60° dihedral angle between 3-H and 3′-H.

graphs of 2-H/3′-CH_3 and 3-H/3′-CH_3 interatomic distances as a function of dihedral angle (defined as 3′-H/C-3′/C-3/3-H) for both the *R** and *S** configurations at C-3′. The observation that the 3′-CH_3/3-H cross peak was more intense than the 3′-CH_3/2-H cross peak was, in itself, suggestive of a dihedral angle greater than 50° in the *R** configuration or 10–20° in the *S** configuration. The calculated interatomic distances for a 50–100° angle in the *R** case would all be less than 3.5 Å, generally considered to be within the limits of observable dipole exchange. In contrast, the *S** analogue's corresponding distances would fall between 3.8 and 4.6 Å, and cross peak intensities in this range would be very weak, if observable at all. This assertion was also supported by an internal consistency of data from other exchange sites. For example, if the configuration at C-3′ was *S** with a dihedral angle of 20°, then the 5-H/3′-CH_3 interaction should be considerably more intense than observed. Furthermore, a small (20°) dihedral angle would not be consistent with the observed coupling constants.

A dihedral angle range of 60–100° best accounts for the observed interactions with the 3*R**,3′*R** relative stereochemistry (Figure 6). This range is also consistent with values obtained from the Karplus curve[31,32] where a 3.9-Hz coupling constant

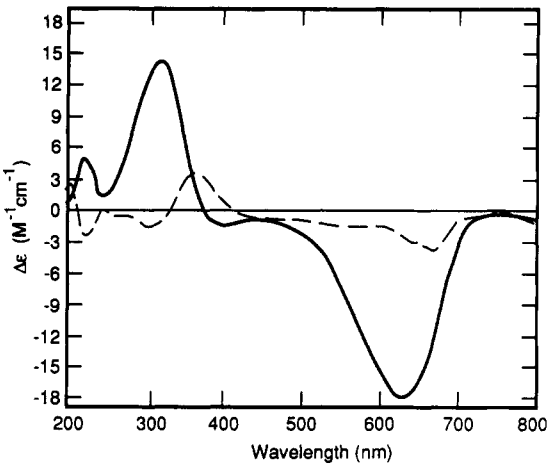

Figure 7. Circular dichroism spectra of **11A** (—) and **11D** (---) in 10 mM aqueous TFA at 23 °C. Both samples were 41 μM in concentration.

would translate roughly to a 75° or 115° dihedral angle.

Circular Dichroism (CD) Spectroscopic Studies. CD spectra for both diastereomers, **11A** and **11D** (Figure 7), were recorded in 10 mM aqueous TFA at identical concentrations (41 μM). Differences between the two synthetic bilin–cysteine adducts are quite pronounced. Diastereomer **11A** exhibits a very intense negative Cotton effect at 634 nm, a strong positive Cotton effect at 324 nm, and a weaker positive Cotton effect at 224 nm. In contrast, the curve obtained from **11D** was relatively flat with comparatively weak peaks in both the visible and UV regions.

Stereochemical Assignments. ^{1}H NMR data demonstrated unambiguously that one diastereomeric bilin–cysteine adduct possessed an absolute stereochemistry of 2*R*,3*R*,3′*R*,Cys-*R* while the other, with an identical relative stereochemistry at C-2/C-3/C-3′, was 2*S*,3*S*,3′*S*,Cys-*R*. These assignments were, additionally, in agreement with mechanistic considerations governing thiolate addition to the bilin group precursor. Unfortunately, it was impossible to relate the known absolute configuration of cysteine to the substituents of the bilin group by using ^{1}H NMR spectroscopy. This, in principle, could have distinguished the two diastereomers and allowed the assignment of **11A** to one absolute configuration and **11D** to the other. Also unsuccessful were efforts to crystallize the synthetic intermediates and products, typically amorphous solids or oils, thus prohibiting assignment of absolute stereochemistry by X-ray crystallography.

Correlation of data to CD spectra reported for the natural product derived bilipeptides does, however, allow a probable assignment of absolute stereochemistry to be made. The CD spectrum of **11A** closely resembles that derived from the β-1 bilipeptide at similar solution concentrations: both have an intense negative Cotton effect in the visible region and a strong positive Cotton effect in the UV region.[23,33] The CD spectrum of **11D** was quite different, showing relatively weak, undefined peaks. Since the β-1 chromophore has been unambiguously shown to possess a 2*R*,3*R*,3′*R* absolute stereochemistry,[4] this assignment is likewise made for **11A**. The unnatural 2*S*,3*S*,3′*S* configuration is thus assigned to **11D**. However, since the relative stereochemistry of diastereomers **11A** and **11D** has been determined by ^{1}H NMR spectroscopy, the task of absolute stereochemistry determination was greatly simplified. Identification of only one stereocenter was necessary, suggesting that a degradation procedure with obliteration of two of the three bilin group stereocenters of **11A** and **11D** may lead to materials more adaptable to configurational analysis.

The literature suggested two possible degradation procedures. The first involved a chromic acid/ammonia, oxidation/elimination

Scheme VI. Degradation of Phycocyanin to Asymmetric Succinimide

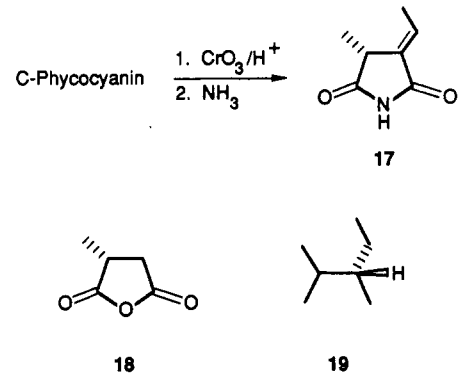

Scheme VII. Convergence of Bilins Released from Synthetic Bilin–Cysteine Adducts and C-Phycocyanin

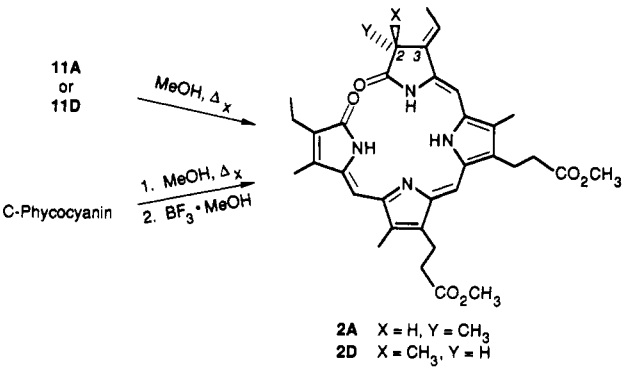

sequence. Assignment of 2*R* stereochemistry had been made for the bilin groups of C-phycocyanin on the basis of the purported isolation of the levorotatory isomer of (*E*)-2-ethylidene-3-methylsuccinimide (**17**) by this method (Scheme VI).[13] This stereoisomer had been previously assigned the *R* configuration.[34] Unfortunately, such an assignment for the chromophores of C-PC was questionable on three counts. First, it was assumed that all three chromophores of C-PC were stereochemically identical. Second, the stereochemical assignment of **17** was based on a series of interconversions of the optically enriched, independently synthesized dextrorotatory isomer of **17** to compounds where chirality had been previously related to (+)-(2*R*)-methylsuccinic anhydride (**18**) and (−)-(3*S*)-2,3-dimethylpentane (**19**).[34] While stereochemistry assignments of the latter two compounds appear secure, reasoning and evidence relating to the assignment of **17** were neither clear nor well-documented. Finally, while it was stated that C-phycocyanin afforded the levorotatory enantiomer of **17**,[13,34] an experimental description of this degradation with physical and analytical data was not presented. Our attempts to preparatively degrade **11A** and **11D** to the enantiomers of **17** under these and other reaction conditions met with failure.

A more successful approach involved β-elimination of the cysteinyl moiety from **11A** and **11D**, which would, in principle, generate enantiomers **2A** and **2D**, respectively (Scheme VII), differing in configuration at C-2. Since the X-ray crystal-structure determinations unequivocally proved the stereochemistry at C-2 for all three C-PC chromophores to be 2*R*,[4] an authentic sample of (2*R*)-**2** might be obtained by a similar release/esterification sequence from the natural product, thus enabling stereochemical assignments to be made for synthetically derived **2A** and **2D**.

Initial release experiments were carried out by treating **11A** with TFA/HBr, which was found to induce the desired elimination reaction in relatively high (>50%) isolated yields. However, the elimination product was found to be completely racemized, as judged by CD spectroscopy. Release of the bilin groups from **11A** and **11D** upon reflux in methanol afforded samples of optically active **2A** and **2D** in approximately 50% yield after purification

(31) Bothner-By, A. A. *Adv. Magn. Reson.* **1965**, *1*, 195.
(32) Becker, E. D. *High Resolution NMR*; Academic Press: New York, 1980; pp 102–105.
(33) Lagarias, J. C.; Glazer, A. N.; Rapoport, H. *J. Am. Chem. Soc.* **1979**, *101*, 5030.
(34) Brockmann, H.; Knobloch, G. *Chem. Ber.* **1973**, *106*, 803.

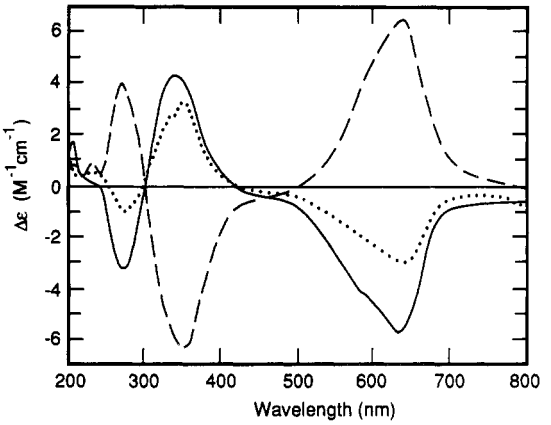

Figure 8. Circular dichroism spectra of **2A** (—), **2D** (---), and **2** derived from natural product (C-PC) degradation (···) in methanol at 23 °C. All samples were 51 μM in concentration.

by silica gel chromatography. The desired products were accompanied by lower R_f methanol addition products.[15] Released PCB groups **2A** and **2D** had identical ^{1}H NMR absorbance and mass spectra but exhibited mirror image CD curves (Figure 8), proving their enantiomeric nature. A ROESY ^{1}H NMR experiment (data not presented) confirmed *Z*-syn geometries between all rings. A suspension of C-phycocyanin was similarly refluxed in methanol, and the resulting filtrate was esterified with BF_3·MeOH. After chromatography, the product was found to be essentially identical with synthetically derived **2A** (Figure 8). The fact that the CD spectrum of naturally derived **2** did not have peaks of the same intensity as synthetically derived **2A** is interpreted as due to partial racemization during the release/esterification reactions. Nonetheless, the qualitative and near-quantitative consistency of CD data with the known C-2 center of the natural product confirms the assignment of 2*R*,3*R*,3′*R* absolute stereochemistry for diastereomer **11A**. It follows that diastereomer D possesses the 2*S*,3*S*,3′*S* arrangement.

Finally, a series of control reactions was performed in order to try to deduce why partial racemization was observed with the natural product cleavage but not with the synthetic tetrapyrroles. The first obvious place to look was at the esterification conditions. Treatment of **2A** with BF_3·MeOH, isolation, and chromatography afforded a material that had sustained no observable racemization, as seen by CD spectroscopy, indicating that BF_3·MeOH was not the culprit. However, extending the reflux time for the natural product in methanol from 26 h to 92 h, with subsequent esterification and isolation, was found to afford **2** with no observable optical activity. Since no such racemization was observed with synthetic bilin–cysteine adduct **11A** upon extended reflux, the attached protein of the natural product must be responsible for the racemization observed.

Conclusions

In comparing the synthetic diastereomers with the natural product derived bilipeptides, nearly identical UV–vis absorption spectra are observed. However, when comparing the synthetic diastereomers with the native protein C-PC, differences are seen. At neutral pH, the visible absorption maximum of C-PC was reported to be 622 nm.[11] In a neutral medium, the absorption maximum of the synthetically derived bilin–cysteine adduct **11A** was approximately 590 nm. As speculated earlier, this may be a result of differing bilin conformations. A comparison of data from the X-ray crystallographic study[4] and the present NMR analysis tend to support this hypothesis. The chromophore in C-PC is in an extended conformation with a *Z*-anti, *Z*-syn, *Z*-anti relationship between rings (Figure 1). The synthetic materials assume a presumably more energetically favorable, helical conformation, with a *Z*-syn, *Z*-syn, *Z*-syn relationship between rings (Scheme III). Such a conformational change may also account for the drastic decrease in fluorescence quantum yield upon denaturation of the protein.[35]

Synthesis is a valuable complement to natural product studies in that relatively large amounts of homogeneous material can be produced and useful chemical manipulations of the pigment can be explored without having to rely on limited amounts of material isolated from the algae. The methodology described in this report should be potentially adaptable to synthesizing more complex natural product analogues, for instance incorporation of an oligopeptide rather than a single cysteine residue and generation of free acid rather than methyl ester bilin groups. This methodology could also be adapted to the synthesis of unnatural materials, differing in well-defined stereochemical or conformational properties with the natural product.

Finally, the value of the ROESY experiment as an analytical tool is clearly evident. For deciphering configuration and solution conformation, ROESY is the NMR experiment of choice. Its advantages over the NOESY experiment include faster acquisition time, cross relaxation rates greater than or equal to NOESY cross relaxation rates, and cross peaks that are always antiphase to the diagonal, thus allowing discrimination of possible spectral artifacts. Use of this combination of synthetic and analytical methodology may be quite effective in further studies of the structure, function, and mechanism of action of these bile pigments.

Experimental Section

General Methods. Acetonitrile, toluene, diisopropylethylamine, and methylene chloride were distilled from CaH_2 before use. Ethanol was distilled from its magnesium salt. Trimethyl orthoformate, DBU, and trifluoroacetic acid (TFA) were distilled before use. Reactions were performed under an atmosphere of nitrogen and were stirred magnetically, unless otherwise noted. Evaporations were done on a Berkeley rotary evaporator using a water aspirator or oil-pump vacuum, followed by static evaporation with an oil-pump vacuum. Kieselgel 60 F_{254} plates (E. Merck) were used for thin-layer chromatography (TLC) while 230–400-mesh silica gel 60 (E. Merck) was used for low-pressure chromatography (LPC). UV–vis and circular dichroism (CD) spectra were recorded with a Perkin-Elmer 522A spectrophotometer and a JASCO J-500C spectrophotometer, respectively, at 23 °C. High-resolution electron-impact (EI) and fast atom bombardment (FAB) mass spectra were obtained on a Kratos MS-50 instrument. The FAB spectra were obtained by applying the sample to a matrix of glycerol/thioglycerol and then scanning at 8 kV with use of xenon gas; elemental compositions were determined by peak matching against glycerol adducts. Melting points were determined on a Büchi capillary melting point apparatus; both melting and boiling points are uncorrected. Elemental analyses were performed by the Analytical Laboratory, College of Chemistry, University of California, Berkeley.

NMR Spectroscopy. ^{1}H NMR spectra were recorded at 500.135 MHz on a Bruker AM 500 spectrometer. Unless noted, all spectra were obtained in $CDCl_3$ with an internal tetramethylsilane standard calibrated to 0.00 ppm. Spectra obtained in pyridine-d_5 were calibrated to the upfield residual pyridine peak at 7.18 ppm. ^{1}H NMR data are tabulated in the following order: chemical shift (δ), multiplicity (s, singlet; d, doublet; t, triplet; q, quartet; m, multiplet), number of protons, and coupling constant(s) in hertz. Coupling constants were derived from 1-D spectra with a minimum digital resolution of 0.15 Hz/point and employment of a sine bell apodization for resolution enhancement. Phase-sensitive NOESY and COSY experiments[22,26] were performed by using standard procedures.

For ROESY spectra,[28] the pulse sequence $\pi/2$–t_1–$(\beta - \tau)_N$–ACQ was used in the inverse mode with the TPPI method. A total of 512 experiments of size 2K with 24 scans each were recorded with an acquisition time of 0.315 s and a relaxation delay of 2 s. The spin-lock field was generated by using small flip angles (17°), β = 1.63 μs, τ = 16.3 μs, and N = 11 150, for a total mixing time of 200 ms and an effective field of 2600 Hz. Typical spectral widths were 3246 Hz in $CDCl_3$ and 4386 Hz in pyridine-d_5. Data were processed by zero filling to 2K in F1 and use of a sine bell apodization in both F1 and F2. Probe temperature during 1-D and 2-D measurements was 22–25 °C.

Computational Methods. The molecular program used was the 1977 MM2 program[36] without π parameters on a MicroVAX system. Required torsional, stretch, and in-plane bending constants not included for the model system were subplanted with generalized constants.

(35) Scheer, H. *Angew. Chem., Int. Ed. Engl.* **1981**, *20*, 241.
(36) (a) Burket, R.; Allinger, N. L. *Molecular Mechanics*; American Chemical Society: Washington, DC, 1982. (b) Allinger, N. L. *J. Am. Chem. Soc.* **1977**, *99*, 8127.

The relaxation matrix calculation program was written in BASIC on an IBM PC. The relaxation matrix was constructed with the transitional probabilities for longitudinal and transverse relaxation. T_1 and T_2 values were calculated by least-squares fitting the natural logarithm of the diagonal elements of the matrix exponential as a function of mixing time to a linear function. A chi-squared analysis was used to evaluate the fit of the relaxation behavior to a single exponential over a range of relaxation times. Optimum mixing times and other relevant parameters were calculated from the experimentally fitted relaxation matrix. Methyl group internal correlation times were evaluated as "fast" ($\tau_c' = \tau_c/4$), "medium" ($\tau_c' = \tau_c/2$), and "slow" ($t_c' = \tau_c$) ranges. Spin systems of interest did not need more elaborate treatment of internal motion. Methyl group internal relaxation was treated both explicitly in the construction of the relaxation matrix from the relevant transition probabilities[27] and indirectly through leakage rates.

The diagonalization of unsymmetrical relaxation matrices due to methyl–proton relaxation was accomplished by first symmetrizing the matrix, diagonalizing,[37] and then unsymmetrizing at the matrix exponential state. The general problem of diagonalizing an unsymmetrical matrix was beyond the scope needed for this work.

2,3-Dihydro-2,7-dimethyl-8-[2-(methoxycarbonyl)ethyl]-3-[3′-((*R*)-*O*-methylcystein-*S*-yl)ethyl]pyrromethenone-5,9-dicarboxylic Acid Di-*tert*-Butyl Ester (6A,B,C,D).[16] A solution of 1.49 g (2.96 mmol) of thio-Wittig adduct **5**[10] and 0.61 g (120 mol %) of L-cysteine methyl ester hydrochloride in 25 mL of CH_3CN was brought to 0 °C; DBU (0.59 mL, 132 mol %) was then added, and the homogeneous solution was stirred for 2.5 h. After concentration, the residue was purified by LPC eluting with hexanes/EtOAc 5/1. The high-R_f material was 0.22 g (15%) of recovered starting material. A medium-R_f product, 0.72 g (38%) of a yellowish foam, contained one major diastereomer (**6A**) and one minor diastereomer (**6B**). The low-R_f product, 0.55 g (29%), was likewise composed of one minor (**6C**) and one major (**6D**) diastereomer. Because the minor diastereomers were present in such small quantities, their spectroscopic characterization was not pursued at this stage. Full characterization was performed after the subsequent acetylation and separation of diastereomers. Only ^{1}H NMR data from the major diastereomers are presented here.

6A: ^{1}H NMR 10.76 (br s, 1 H), 10.48 (br s, 1 H), 3.72 (s, 3 H), 3.67 (s, 3 H), 3.56 (t, 1 H, J = 6.2), 2.94–3.10 (m, 3 H), 2.85 (br m, 1 H), 2.68 (br m, 1 H), 2.51–2.55 (m, 3 H), 2.45 (br m, 1 H), 1.90 (s, 3 H), 1.56 (s, 9 H), 1.42 (s, 9 H), 1.29 (d, 3 H, J = 7.5), 1.13 (d, 3 H, J = 6.9).

6D: ^{1}H NMR 10.41 (br s, 1 H), 10.26 (br s, 1 H), 3.74 (s, 3 H), 3.67 (s, 3 H), 3.59 (t, 1 H, J = 6.4), 2.93–3.10 (m, 3 H), 2.89 (br m, 1 H), 2.74 (br m, 1 H), 2.51–2.54 (m, 4 H), 1.90 (s, 3 H), 1.56 (s, 9 H), 1.43 (s, 9 H), 1.28 (d, 3 H, J = 7.5), 1.10 (d, 3 H, J = 6.9).

2,3-Dihydro-2,7-dimethyl-3-[3′-((*R*)-*N*-acetyl-*O*-methylcystein-*S*-yl)ethyl]-8-[2-(methoxycarbonyl)ethyl]pyrromethenone-5,9-dicarboxylic Acid Di-*tert*-Butyl Ester (7A,B,C,D).[16] The medium-R_f mixture of diastereomers **6A** and **6B** (0.72 g, 1.13 mmol) was dissolved in 15 mL of CH_2Cl_2 and brought to approximately 0 °C. Acetic anhydride (123 μL, 115 mol %) was added, the mixture was stirred for 10 min, an additional 10 mL of CH_2Cl_2 was added, and the solution was washed with saturated aqueous $NaHCO_3$ (2 × 10 mL). Each aqueous layer was back-extracted with CH_2Cl_2 (2 × 5 mL). The combined organic layers were washed with saturated NaCl (10 mL), dried over $MgSO_4$, filtered, and concentrated. Chromatography of the residue using hexanes/EtOAc 4/1 (later fractions were eluted with hexane/EtOAc 1/1) afforded 0.63 g (82%) of the major high R_f diastereomer **7A** and 0.15 g (19%) of a lower R_f diastereomer **7B**, both as yellowish foams.

7A: ^{1}H NMR 10.47 (br s, 1 H), 10.41 (br s, 1 H), 6.61 (br s, 1 H), 4.76 (q, 1 H, J = 7.5), 3.73 (s, 3 H), 3.67 (s, 3 H), 3.09–3.12 (m, 1 H), 2.95–3.04 (m, 1 H), 2.81 (d, 2 H, J = 6.3), 2.73 (br s, 1 H), 2.50–2.55 (m, 4 H), 1.96 (s, 3 H), 1.90 (s, 3 H), 1.56 (s, 9 H), 1.44 (s, 9 H), 1.28 (d, 3 H, J = 7.5), 1.10 (d, 3 H, J = 6.8); high-resolution EI MS m/z calcd for $C_{33}H_{49}N_3O_{10}S$ (M^+) 679.3139, found 679.3158.

7B: ^{1}H NMR 10.40 (br s, 1 H), 8.72 (br s, 1 H), 6.22 (br s, 1 H), 4.55 (q, 1 H, J = 7.0), 3.74 (s, 3 H), 3.69 (s, 3 H), 3.00 (m, 2 H), 2.80 (br m, 1 H), 2.46–2.59 (m, 6 H), 2.01 (s, 3 H), 1.90 (s, 3 H), 1.57 (s, 9 H), 1.41 (s, 9 H), 1.34 (d, 3 H, J = 7.4), 0.98 (d, 3 H, J = 7.1); high resolution EI MS m/z calcd for $C_{33}H_{49}N_3O_{10}S$ (M^+) 679.3139, found 679.3151.

The 0.55-g (0.862 mmol) sample of diastereomers **6C** and **6D** was treated as described above. Chromatography was performed with hexanes/EtOAc as eluant in a gradient of 10/1 to 1/1. The slightly higher R_f diastereomer **7C** (0.03 g, 5%) was obtained as a yellow oil, and the major diastereomer **7D** (0.43 g, 74%) was a yellowish foam.

7C: ^{1}H NMR 10.37 (br s, 2 H), 6.36 (br d, 1 H, J = 7.5), 4.70 (br q, 1 H, J = 7.6), 3.74 (m, 3 H), 3.67 (s, 3 H), 3.18 (br m, 1 H), 3.06–3.12 (m, 1 H), 2.95–3.01 (m, 1 H), 2.72–2.79 (m, 4 H), 2.57 (t, 2 H, J = 7.3), 1.97 (s, 3 H), 1.91 (s, 3 H), 1.56 (s, 9 H), 1.42 (s, 9 H), 1.37 (d, 3 H, J = 7.4), 1.16 (d, 3 H, J = 7.4); high resolution EI MS m/z calcd for $C_{33}H_{49}N_3O_{10}S$ (M^+) 679.3139, found 679.3143.

7D: ^{1}H NMR 10.39 (br s, 1 H), 9.87 (br s, 1 H), 6.38 (br s, 1 H), 4.63 (br s, 1 H), 3.76 (s, 3 H), 3.66 (s, 3 H), 2.95–3.09 (m, 3 H), 2.77 (m, 2 H), 2.49–2.55 (m, 4 H), 2.03 (s, 3 H), 1.90 (s, 3 H), 1.57 (s, 9 H), 1.43 (s, 9 H), 1.29 (d, 3 H, J = 7.5), 1.09 (d, 3 H, J = 7.1); high resolution EI MS m/z calcd for $C_{33}H_{49}N_3O_{10}S$ (M^+) 679.3139, found 679.3155.

(2*R*,3*R*,3′*R*)-2,3-Dihydro-2,7-dimethyl-3-[3′-((*R*)-*N*-acetyl-*O*-methylcystein-*S*-yl)ethyl]-8-[2-(methoxycarbonyl)ethyl]-9-formylpyrromethenone-5-carboxylic Acid (8A).[16] A solution of 0.63 g (0.93 mmol) of **7A** in 6 mL of CH_2Cl_2 was brought to 0 °C, and 6 mL of TFA was added. The reaction was then stirred for 3 h at room temperature, after which 6 mL of trimethyl orthoformate was rapidly added. After 10 min, the reaction mixture was transferred to a flask containing 35 mL of H_2O at 0 °C and basified to pH 8 by incremental additions of solid $NaHCO_3$. After the layers were separated, the aqueous layer was washed with CH_2Cl_2 (2 × 5 mL), chilled to 0 °C, CH_2Cl_2 (10 mL) was added, the solution was acidified to pH 2 with 85% (wt/wt) H_3PO_4, and the phases were separated. After washing with CH_2Cl_2 (8 × 20 mL), the combined organic extracts were washed with 5 mL of saturated NaCl, dried over $MgSO_4$, filtered, and concentrated, affording 0.44 g (86%) of a pink solid that was used without further purification in the next reaction. Extensive line broadening and possible partial double bond isomerization made ^{1}H NMR assignments impossible. High-resolution FAB MS m/z calcd for $C_{25}H_{34}N_3O_9S$ (MH^+) 552.2016, found 552.2007.

(2*S*,3*S*,3′*S*)-2,3-Dihydro-2,7-dimethyl-3-[3′-((*R*)-*N*-acetyl-*O*-methylcystein-*S*-yl)ethyl]-8-[2-(methoxycarbonyl)ethyl]-9-formylpyrromethenone-5-carboxylic Acid (8D).[16] A 100.1-mg (0.1472 mmol) sample of **7D** was treated in the same manner as was **7A**, affording 60.2 mg (74%) of **8D** as a pink solid, that was used without further purification in the next reaction. Extensive line broadening and possible partial double bond isomerization prevented ^{1}H NMR assignments. High-resolution FAB MS m/z calcd for $C_{25}H_{34}N_3O_9S$ (MH^+) 552.2016, found 552.2013.

(2*R*,3*R*,3′*R*)-3,3′-Dihydro-8,12-di-[2-(methoxycarbonyl)ethyl]-3′-((*R*)-*N*-acetyl-*O*-methylcystein-*S*-yl)phycocyanobilin-5-carboxylic Acid (10A). A solution of 75.3 mg (0.249 mmol) of pyrromethenone **9** (see Discussion) and 151.2 mg (110 mol %) of diastereomer **8A** in 15 mL of CH_2Cl_2 and 10 mL of CH_3CN was brought to approximately 0 °C, and 10 drops of 33% (wt/wt) HBr in acetic acid were added with a 5.75-in. Pasteur pipet. The mixture instantly developed a blue color and gradually became homogeneous. After 1 h, 2 h, and 3 h, additional 10-drop aliquots of 33% (wt/wt) HBr/HOAc were added. After 3.5 h, yellow-colored **9** was no longer detectable by TLC (EtOAc). The solution was concentrated (bath temperature <35 °C), redissolved in 35 mL of $CHCl_3$, and washed with saturated $NaHCO_3$ (2 × 30 mL), H_2O (20 mL), and saturated NaCl (20 mL). Each aqueous layer was washed with $CHCl_3$ (2 × 10 mL), and the combined organic layers were concentrated leaving 249.8 mg of a blue solid. Attempted chromatographic purification for full characterization by ^{1}H NMR resulted in extensive decomposition, so the crude material was used with only minimal characterization in the next reaction: UV–vis (MeOH) λ_{max} 332, 572 nm; UV–vis (10 mM aqueous TFA) λ_{max} 326, 597 nm; high-resolution FAB MS m/z calcd for $C_{42}H_{54}N_5O_{11}S$ (MH^+) 836.3541, found 836.3541.

(2*S*,3*S*,3′*S*)-3,3′-Dihydro-8,12-di-[2-(methoxycarbonyl)ethyl]-3′-((*R*)-*N*-acetyl-*O*-methylcystein-*S*-yl)phycocyanobilin-5-carboxylic Acid (10D). A 60.2-mg (0.109 mmol) sample of **8D** was treated in the same manner as described for **8A**, affording 100.1 mg of crude product that was used directly in the next reaction. FAB MS m/z calcd for $C_{42}H_{54}N_5O_{11}S$ (MH^+) 836.3541, found 836.3564.

(2*R*,3*R*,3′*R*)-3′-((*R*)-*N*-Acetyl-*O*-methylcystein-*S*-yl)-3,3′-dihydrophycocyanobilin Dimethyl Ester (11A). Crude tetrapyrrolecarboxylic acid **10A** (0.25 g) was dissolved in 100 mL of toluene, and 10 mL of diisopropylethylamine was added. The reaction vessel, equipped with a condenser, was heated to 105 °C (bath temperature) under a static atmosphere of argon in the dark for 14.5 h; TLC (EtOAc) showed no remaining starting material and two higher R_f product spots. The solution was concentrated under reduced pressure (2.0 mm) with a bath temperature of approximately 35 °C. The residue was redissolved in 50 mL of EtOAc and reconcentrated. Chromatography was performed on a 3.5 × 23 cm silica column, eluting rapidly with EtOAc.

The least polar material (R_f = 0.70) was blue in color and was identified as 0.02 g (13% based on **9**; 2 steps) of elimination product **2**.[38] For

(37) Golub, G. H.; Van Loan, C. F. *Matrix Computations*; Johns Hopkins University Press: Baltimore, MD, 1983.

(38) Gossauer, A.; Hirsch, W. *Liebigs Ann. Chem.* **1974**, 1496.

full characterization see the following.

The major product (R_f = 0.34), identified as desired product **11A**, was obtained as 0.18 g (91% based on **9**; 2 steps) of a purple-colored solid. For stereochemical and conformational assignments see Discussion. UV–vis (MeOH): λ_{max} (log ϵ): 590 (4.24), 345 (4.58), 273 (0.76), 202 (0.68) nm; see Figure 2. UV–vis (10 mM aqueous TFA): λ_{max} (log ϵ) 647 (4.50), 347 (4.53), 2.82 (sh), 196 (4.27) nm; see Figure 2. ^{1}H NMR ($CDCl_3$): see Table I and Figure 3. ^{1}H NMR (pyridine-d_5): see Table II and Figure 4. CD spectrum (10 mM aqueous TFA): see Figure 7. High-resolution FAB MS m/z: calcd for $C_{41}H_{54}N_5O_9S$ (MH^+) 792.3642, found 792.3672. Anal. Calcd for $C_{41}N_{53}N_5O_9S$: C, 62.2; H, 6.8; N, 8.8. Found: C, 61.9; H, 6.9; N, 8.5.

In some experiments, varying amounts of oxidation product **12A** were also observed by TLC as a blue spot slightly higher in R_f (0.38) than the major, purple-colored product. High-resolution FAB MS m/z calcd for $C_{41}H_{52}N_5O_5S$ (MH^+) 790.3486, found 790.3452. See Discussion for ^{1}H NMR information.

(2*S*,3*S*,3′*S*)-3′-((*R*)-*N*-Acetyl-*O*-methylcystein-*S*-yl)-3,3′-dihydrophycocyanobilin Dimethyl Ester (11D). Crude tetrapyrrolecarboxylic acid **10D** (0.10 g) was treated in a manner analogous to **10A** and purified by LPC on a 2.3 × 20 cm silica column. Separation from the contaminating elimination and oxidation products afforded 17.2 mg (18% based on **9**; 2 steps) of a purple-colored solid. For stereochemical and conformational assignments, see Discussion. UV–vis (MeOH): λ_{max} (log ϵ) 689 (4.29), 345 (4.62), 273 (4.32), 202 (4.35) nm. UV–vis (10 mM aqueous TFA): λ_{max} (log ϵ) 647 (4.52), 346 (4.57), 282 (sh), 197 (4.30) nm. ^{1}H NMR ($CDCl_3$): see Table I. ^{1}H NMR (pyridine-d_5): see Table II. CD spectrum (10 mM aqueous TFA): see Figure 7. High-resolution FAB MS m/z: calcd for $C_{41}H_{54}N_5O_9S$ (MH^+) 792.3642, found 792.3643.

Ethyl 2-Ethyl-3-oxobutanoate (13). This product was prepared by major modifications of the reported procedure.[3,39] Sodium metal (23.1 g, 1.00 mol) was added to 800 mL of dry ethanol. After the sodium had been totally consumed, ethyl acetoacetate (127 mL, 100 mol %) was added all at once, and the mixture was warmed to 80 °C. Ethyl iodide (80.0 mL, 100 mol %) was added dropwise over a 2-h period, and the reaction mixture was kept at 80 °C for an additional 2 h, after which the ethanol was evaporated. A 500-mL portion of EtOAc was added and the slurry was filtered. After the solid was washed with EtOAc (2 × 100 mL), the combined filtrates were concentrated and applied to a 6 × 60 cm silica column. After eluting with hexanes/EtOAc 9/1, the desired, marginally lower R_f monoalkylated material **13** could be removed almost entirely (>98% by ^{1}H NMR integration) from the undesired dialkylated material **14** by examining fractions by TLC (hexanes/EtOAc 1/1). A clear liquid (82.5 g, 52%) was obtained: ^{1}H NMR 4.20 (q, 2 H, J = 6.6), 3.34 (t, 1 H, J = 7.3), 2.23 (s, 3 H), 1.89 (m, 2 H, J = 7.6), 1.28 (t, 3 H, J = 7.1), 0.94 (t, 3 H, J = 7.4). Anal. Calcd for $C_8H_{14}O_3$: C, 60.7, H, 8.9. Found: C, 60.5; H, 8.8.

The minor dialkylated product **14** could not be isolated completely free of monoalkylated **13**: ^{1}H NMR 4.19 (q, 2 H, J = 6.7), 2.12 (s, 3 H), 1.92 (m, 4 H, J = 6.8), 1.26 (t, 3 H, J = 6.9), 0.76 (t, 6 H, J = 7.6). The percent composition of samples was estimated by comparing intensities of the triplet at 0.94 ppm for monoalkylated **13** versus the triplet at 0.74 ppm for dialkylated **14**.

3-Ethyl-4-methyl-3-pyrrolin-2-one (16). Compound **16** was also prepared by major modifications of the reported procedure.[3,39] β-Keto ester **13** (30.0 g, 190 mmol) was added to a solution of 24.5 g (123 mol %) of $NaHSO_3$ in 50 mL of H_2O. The mixture was brought to 0 °C, and a solution of 18.5 g (199 mol %) of NaCN in 45 mL of H_2O was added dropwise over 15 min, after which the solution was brought to room temperature for 3 h. Additional H_2O (80 mL) was added, and the solution was transferred to a separatory funnel. After removal of the aqueous layer, the organic phase was washed with 5 M H_2SO_4 (2 × 40 mL). The cloudy liquid, 34.25 g, was used immediately in the next reaction.

The crude cyanohydrin was then dissolved in 20 mL of acetic anhydride, and 5 scoops of freshly generated T-1 Raney nickel[21] (ca. 1 g of metal in a slurry with absolute EtOH) were added. After 15 min, the metal was removed by filtration through a bed of Celite, and the filtrate was transferred to a Parr hydrogenation vessel. The volume was increased to approximately 100 mL by adding acetic anhydride, and then 5 scoops of fresh T-1 Raney nickel were added. The mixture was hydrogenated with vigorous shaking at 50 psi and 33 °C. After hydrogen consumption had ceased (12 h), the solution was filtered through Celite and then brought to reflux for 8 h. Concentration afforded a residue, which was dissolved in 250 mL of H_2O. After the addition of 23 g of Na_2CO_3, the solution was refluxed for 4 h, concentrated, and the oily residue was triturated repeatedly (15 × 25 mL) with hot benzene. The combined benzene extracts were concentrated and the residue was distilled with a Kugelrohr apparatus (100–120 °C; 1.5 mm), affording a yellowish solid that was then recrystallized from Et_2O to give 6.81 g (29% based on **13**) of a white powder: mp 101–102 °C (lit.[39] mp 102 °C); ^{1}H NMR 7.69 (br s, 1 H), 3.80 (s, 2 H), 2.27 (q, 2 H, J = 7.6), 1.99 (s, 3 H), 1.07 (t, 3 H, J = 7.6).

Methanolysis of 11A to 2A. A solution of 14.9 mg (18.8 μmol) of **11A** in 20 mL of methanol (undistilled) was brought to reflux (bath temperature 67 °C) under Ar in the dark with magnetic stirring for 26 h. The least polar, blue-colored material (TLC: EtOAc, R_f = 0.62) was isolated by concentrating the reaction mixture and then purifying by LPC (2.5 × 23 mm; hexanes/EtOAc 1/1); it was identified as **2A** (57%). Spectral characteristics were similar to literature values:[38] UV–vis (MeOH) λ_{max} (log ϵ) 614 (4.22), 630 (4.66), 270 (4.21), 202; ^{1}H NMR (pyridine-d_5; squared sine bell apodization) 7.03 (s, 1 H, 10-H), 6.33 (dq, 1 H, J = 7.3, 2.4, 3′-H), 6.07 (s, 1 H, 15-H), 5.86 (s, 1 H, 5-H), 3.61 (s, 3 H, OCH_3), 3.57 (s, 3 H, OCH_3), 3.35 (ddd, 1 H, J = 7.5, 2.4, 1.4, 2-H), 3.06 (t, 2 H, J = 7.4, 12-CH_2CH$_2$CO$_2$CH$_3$), 2.97 (t, 2 H, J = 7.5, 8-CH_2CH$_2$CO$_2$CH$_3$), 2.68 (t, 2 H, J = 7.3, 12-CH$_2$CH_2CO$_2$CH$_3$), 2.65 (t, 2 H, J = 7.7, 8-CH$_2$CH_2CO$_2$CH$_3$), 2.48 (m, 2 H, J = 7.7, 18-CH_2CH$_3$), 2.09 (s, 3 H, 17- or 13-CH$_3$), 2.08 (s, 3 H, 17- or 13-CH$_3$), 1.96 (s, 3 H, 7-CH$_3$), 1.69 (dd, 3 H, J = 7.4, 1.4, 3′-CH$_3$), 1.47 (d, 3 H, J = 7.5, 2-CH$_3$), 1.24 (t, 3 H, J = 7.6, 18-CH$_2$CH_3); for CD spectrum (in MeOH), see Figure 8; high-resolution FAB MS m/z calcd for $C_{35}H_{43}N_4O_6$ (MH^+) 615.3183, found 615.3168.

A minor purple-colored product at R_f = 0.58 was obtained and identified as a methanol addition product.[15]

Methanolysis of 11D to 2D. Compound **11D** was subjected to the refluxing methanol conditions described above affording **2D**, which was indistinguishable, except by its CD spectrum (Figure 8), from **2A**.

Methanolysis of C-Phycocyanin. *Anabaena variabilis* C-Phycocyanin (0.50 g; 13.7 μmol lyophilized protein)[40] was suspended in 200 mL of methanol (undistilled) and heated to reflux (bath temperature, 78 °C) for 26 h in the dark under Ar with magnetic stirring. After filtration and concentration, the blue-colored residue was dissolved in 5 mL of 14% (wt/wt) BF_3·MeOH, and the solution was heated to 78 °C (bath) for 3 min under Ar. Chloroform (10 mL) and 100 mL of H_2O were added, and after the layers were separated, the aqueous layer was washed with $CHCl_3$ (3 × 15 mL). The combined organic extracts were concentrated and purified by LPC as described for **2A**. The major product (TLC: EtOAc, R_f = 0.64) was indistinguishable from **2A** by TLC, ^{1}H NMR, UV–vis, and FAB mass spectroscopy. For the CD spectrum (in MeOH) see Figure 8.

A minor, purple-colored product at R_f = 0.58 was identified as a methanol addition product.[15]

Acknowledgment. This research was supported in part by Grant GM 28994 awarded by the National Institute of General Medical Sciences, DHHS.

Registry No. 2A, 21063-32-1; **2D**, 135682-79-0; **5**, 135145-06-1; **6A**, 135684-14-9; **6B**, 135614-47-0; **6C**, 135684-15-0; **6D**, 135682-80-3; **7A**, 135614-48-1; **7B**, 135682-81-4; **7C**, 135682-82-5; **7D**, 135682-83-6; **8A**, 135614-49-2; **8D**, 135682-84-7; **9**, 13129-09-4; **10A**, 135614-50-5; **10D**, 135684-16-1; **11A**, 135614-51-6; **11D**, 135682-85-8; **12A**, 135614-52-7; **12D**, 135682-86-9; **13**, 607-97-6; **14**, 1619-57-4; **16**, 766-36-9; H-Cys-OMe·HCl, 18598-63-5; CH_3COCH_2COOEt, 141-97-9.

Supplementary Material Available: Calculations (MM2) for the *R*-3′ center stereochemistry and *S*-3′ center stereochemistry internuclear distances as a function of the 3′H/5H, 3H/3′H, and 3H/5H dihedral angles (2 pages). Ordering information is given on any current masthead page.

(39) Plieninger, H.; Decker, H. *Liebigs Ann. Chem.* **1956**, *598*, 198.

(40) Bryant, D. A.; Glazer, A. N.; Eiserling, X. Y. *Arch. Microbiol.* **1976**, *110*, 61.